

DSC, X-ray and magnetic studies on electroless Ni–P films grown in alkaline ethanolamine baths

K. S. Rajam, Indira Rajagopal and S. R. Rajagopalan

Materials Science Division, National Aeronautical Laboratory, Bangalore 560 017 (India)

B. Viswanathan

Department of Chemistry, Indian Institute of Technology, Madras 600 036 (India)

(Received April 13, 1992; accepted August 3, 1992)

Abstract

Results of XRD and DSC studies on electroless Ni–P deposits obtained from two types of alkaline baths containing ethanolamines are discussed. One type (called CT-EN) employed citrate as a complexant, while the other (GE-EN) used glycine as a complexant. GE-EN baths gave an amorphous deposit even at a low phosphorus content (4.8 wt.%), while deposits from CT-EN baths exhibited an amorphous nature only above 9% P. Densities of GE-EN deposits were lower than those of CT-EN deposits of similar phosphorus content. Thermograms of deposits from both baths gave a lower temperature exothermic peak. Deposits from GE-EN baths showed a splitting of the low-temperature peak. Through measurement of the saturation magnetic moment of deposits heated at temperatures corresponding to the low-temperature peak, it is shown that the exothermic processes responsible for this peak are crystallization of nickel and reorganization of the amorphous matrix. The possible reasons for the splitting are discussed. The high-temperature peak is shown to be due to formation of Ni + Ni₃P.

Introduction

During detailed investigations on the possibility of using ethanolamines in place of ammonia in the alkaline electroless Ni–P system [1–3], we found that deposits obtained from glycine–triethanolamine exhibited interesting properties. The Ni–P deposit produced from this bath was found to be ‘amorphous’ (as judged from XRD) in the as-plated condition, even though the P content was only 4.8 wt.%. This is surprising, because Ni–P deposits containing the same amount of P (4.3 wt.%) produced from citrate–triethanolamine were found to be crystalline in the as-plated condition. The properties of Ni–P deposits from the glycine–triethanolamine system (GT-EN) were also markedly different from those of Ni–P deposits from the citrate–triethanolamine system (CT-EN). The density of the former was 7.3 g cm⁻³, while that of the latter was 8.45 g cm⁻³. A similar difference was observed in their microhardness values: GT-EN deposits exhibited a hardness value of 300 VHN, whereas CT-EN deposits were found to be harder, with a hardness value of 525 VHN. These interesting observations prompted us to undertake a detailed structural

investigation, and the results of these studies are presented in this paper.

Experimental

Citrate- or glycine-based baths containing ethanolamine, developed by the authors [1–3], were used to prepare electroless nickel films/samples for XRD (X-ray diffraction), DSC and magnetization studies. GR grade chemicals (Merck) were used for preparing all solutions. The bath compositions and operating conditions are given in Tables 1 and 2. Deposits with different phosphorus contents were prepared from a citrate–triethanolamine bath by varying the concentration of sodium citrate. Deposits from citrate–triethanolamine baths were designated as CT-EN.

TABLE 1. Composition of citrate-based ethanolamine bath

Nickel chloride	0.1 M
Sodium hypophosphite	0.093 M
Sodium citrate	0.15 M
Triethanolamine	0.15 M
Temperature	90 °C

TABLE 2. Composition of glycine-based ethanolamine baths

Nickel chloride	0.1 M
Sodium hypophosphite	0.28 M
Glycine	0.4 M
Ethanolamine (mono, di and tri)	0.3 M
Temperature	90 °C

Characterization studies were undertaken for CT-EN deposits with 4.3, 9, 12.5 and 15.5 wt.% P, and these deposits were designated as deposits 1, 2, 3 and 4 respectively.

Deposits from glycine-ethanolamine were designated as GM-EN, GD-EN and GT-EN, where M, D and T stand for mono-, di- and triethanolamine. These deposits were designated as deposits 5, 6 and 7, respectively.

The phosphorus contents of these EN deposits were determined by a spectrophotometric method. The procedure involves the formation of yellow phosphomolybdate complex and measuring the absorbance at 410 nm. The accuracy of this method is $\pm 1\%$; the details are given elsewhere [3].

The density of the EN deposits was determined by the specific gravity bottle method, using toluene as the liquid.

For XRD studies, EN was deposited on brass substrates. The thickness of the deposit was kept to around 15–20 μm to avoid diffraction lines from the substrate. The diffractograms were recorded using a Philips diffractometer (model PW 1050/70) and a Philips generator (model PW 1730). Cu $K\alpha$ radiation with a graphite monochromator was used.

For DSC and magnetization studies, the EN deposit was used in powder form. For this purpose EN was deposited on polished stainless-steel substrates. The coating was peeled off and ground in an agate mortar to produce the powder. The DSC measurements were made using a Perkin-Elmer differential scanning calorimeter (model DSC-2). The magnetic moment measurements were carried out at room temperature (27 °C) employing an EG&G vibration sample magnetometer (PAR model 155).

For heat treatment studies, the samples were sealed in evacuated (pressure less than 10^{-5} torr) glass tubes and heated in a tubular resistance-heated furnace at the required temperature for 30 min. After heating, the glass tube was removed from the furnace and allowed to cool to room temperature. It was then broken, and the sample

was extracted and used for DSC and magnetization studies.

Results and discussion

Density measurements

The densities of various EN deposits are given in Table 3. It is well known that the density of EN decreases with increasing P content [4]. The Table reveals an interesting fact: the densities of EN deposited from the glycine-ethanolamine bath are seen to be lower than those obtained from the citrate-TEA bath. For instance, deposit 7 [GT-EN (4.8P)] has a density of 7.3 g cm^{-3} , while deposit 1 [CT-EN (4.3P)] has a density of 8.45 g cm^{-3} . The two deposits have a similar P content but widely different densities. It is surprising that the density of deposit 7, from the glycine bath, is nearly the same as that of deposit 4 [CT-EN (15.5P)]. From this observation it can be inferred that glycine deposits are less densely packed or that the deposits contain voids.

XRD studies of EN deposited from ethanolamine baths in the as-deposited condition

The diffractogram of deposit 1 [CT-EN (4.3P)], shown in Fig. 1(a), is seen to consist of lines due to crystalline nickel. However, the intensity of the (200) reflection is seen to be much smaller than that expected based on the fact that the ratio of (111) to (200) should be 1:0.42 [5]. This is indicative of a preferred orientation of the crystallites. No lines due to any phosphide of nickel are seen. In the light of these observations it can be concluded that low-phosphorus CT-EN is supersaturated phosphorus in crystalline nickel. This result agrees with the reported structure of acid citrate EN and ammoniacal citrate EN [6, 7] and electrodeposited Ni-P [8].

The XRD pattern of deposit 2 (CT-EN containing 9 wt.% P) is shown in Fig. 1(b). Deposits 3 and 4, with a higher phosphorus content, gave

TABLE 3. Composition and density of EN deposits

Deposit no	Deposit description	Density (g cm^{-3})
1	CT-EN (4.3 wt.% P)	8.45
2	CT-EN (9 wt.% P)	7.90
3	CT-EN (12.5 wt.% P)	7.60
4	CT-EN (15.5 wt.% P)	7.20
5	GM-EN (6.4 wt.% P)	7.00
6	GD-EN (6.4 wt.% P)	7.00
7	GT-EN (4.8 wt.% P)	7.30

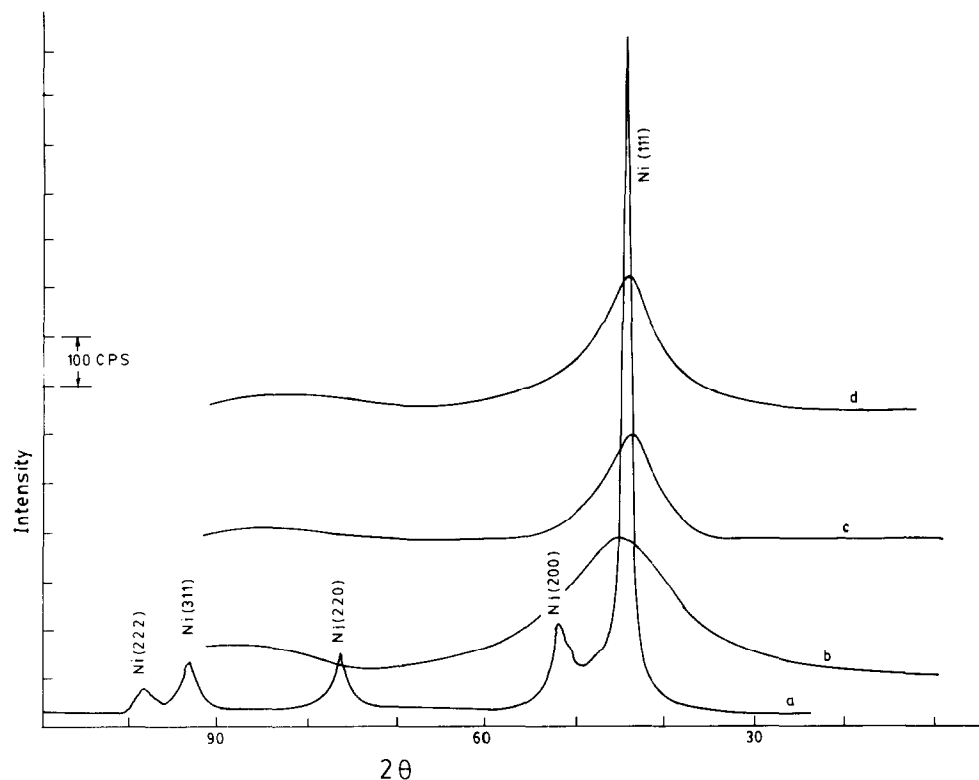


Fig. 1. XRD pattern of as-deposited (a) CT-EN (4.3P); (b) CT-EN (9P); (c) GT-EN (4.8P); (d) XRD pattern of heat-treated GT-EN (4.8P) (at T_{LP} for 15 min).

patterns similar to that of deposit 2. They are characterized by a very broad reflection with a maximum at 2θ close to the Ni(111) line, i.e., $44^\circ 30'$ (for Cu $K\alpha$ radiation), and a weaker and broader reflection on the high-angle side.

The XRD patterns of deposit 5 [GM-EN (6.4P)] and deposit 6 [GD-EN (6.4P)] were similar to that of deposit 7 [GT-EN (4.8P)], which is shown in Fig. 1(c). This closely resembles the diffractogram of CT-EN deposits containing more than 9 wt.% P.

These broadened XRD patterns may be interpreted in one of two ways: they may be considered to be due to small particle size; alternatively, they may be taken to represent the amorphous nature of the deposit.

Following several authors [9–12] we conclude that, with the exception of CT-EN (4.3P), all the deposits are amorphous, for the following reasons:

(i) The diffractogram shows a pronounced broad peak and a very small broadened second maximum, which is characteristic of the diffraction pattern of amorphous material.

(ii) Considering the deposit to be a mixture of Ni and Ni_3P , the percentage of metal in the deposit, estimated from the diffraction peak [13], is found to have a highly improbable value (greater than

100%). Hence the deposit is not a mixture of crystalline phases.

(iii) Estimates of the grain size from line breadths result in unacceptably small values.

XRD studies of heat-treated EN

Figure 2(a) and (b) shows the XRD of CT-EN deposits (4.3 and 9% P) heated in vacuum at 400°C for 1 h. The diffractograms of heat-treated CT-EN (12.5P) and CT-EN (15.5P) are identical to that shown in Fig. 2(b). The various lines could be indexed as being due to nickel and nickel phosphide, which is most probably Ni_3P . Higgs [14] has reported the presence of Ni_7P_3 ($Ni_{12}P_5$) in heat-treated EN. The presence of $Ni_{12}P_5$, Ni_5P_2 and Ni_3P in heat-treated EN has been shown by electron diffraction studies [15–17]. Many of the d values of Ni_5P_2 (hex) and $Ni_{12}P_5$ (b.c.t.) overlap with those of Ni_3P (b.c.t.). Therefore an unambiguous identification of the phosphide phase is difficult. However, it is generally accepted that heat-treated EN contains Ni and Ni_3P . Pittermann and Ripper [18] and Bakonyi *et al.* [19] showed that for EN containing <25 at.% P the phases present after heat treatment are Ni and Ni_3P . However, the present study shows that heat-treated EN deposits with even 25.78 at.% P (15.5 wt.% P) contain Ni_3P .

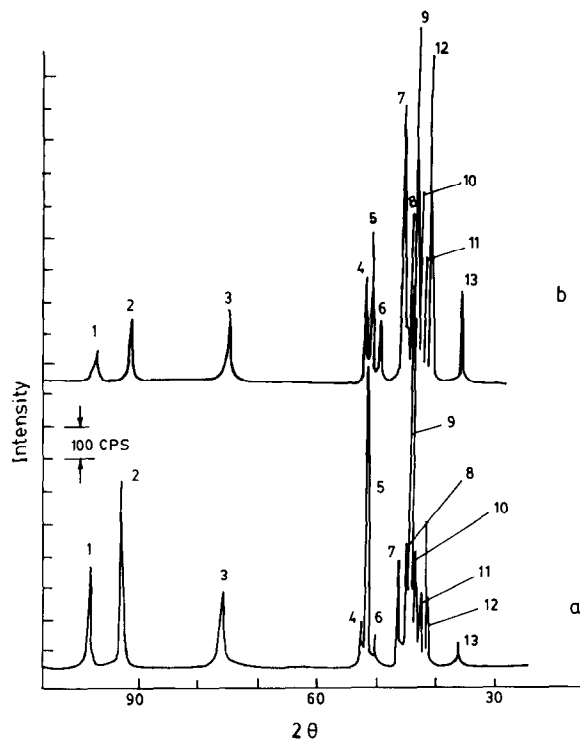


Fig. 2. XRD pattern of heat-treated (400 °C, 1 h) (a) CT-EN (4.3P), (b) CT-EN (9P). The peaks correspond to: 1 - Ni(222); 2 - Ni(311); 3 - Ni(220); 4 - Ni₃P(312); 5 - Ni(200); 6 - Ni₃P(222); 7 - Ni₃P(411); 8 - Ni₃(420); 9 - Ni(111); 10 - Ni₃P(112); 11 - Ni₃P(300); 12 - Ni₃P(321); 13 - Ni₃P(301).

The XRD patterns of heat-treated (400 °C, 1 h) GM-EN, GD-EN and GT-EN are similar to that shown in Fig. 2(b). These patterns could be indexed as being due to Ni and Ni₃P.

DSC studies on EN

Differential scanning calorimetric studies on EN deposited from CT and GE baths were undertaken, since they can throw light on the thermal stability of the deposits.

Thermograms of CT-EN (recorded at scan rates of 10 and 20 K min⁻¹) exhibit only exotherms that are irreversible. As can be seen from Fig. 3 (curves 1 and 2), low-phosphorus deposits CT-EN (4.3P) and CT-EN (9P) show two peaks, one at lower temperature and another at higher temperature. The peak at lower temperature is small and broad. It is barely perceptible in the case of the 4.3% P deposit, whereas it is significant for the 9% P deposit.

Thermograms of deposits containing 12.5% P and 15.5% P are shown in Fig. 3, curves 3 and 4. These exhibit only one irreversible peak at higher temperature. The lower-temperature peak seen for CT-EN with 4.3% P and 9% P (Fig. 3, curves 1 and 2) is absent in the DSC of deposits

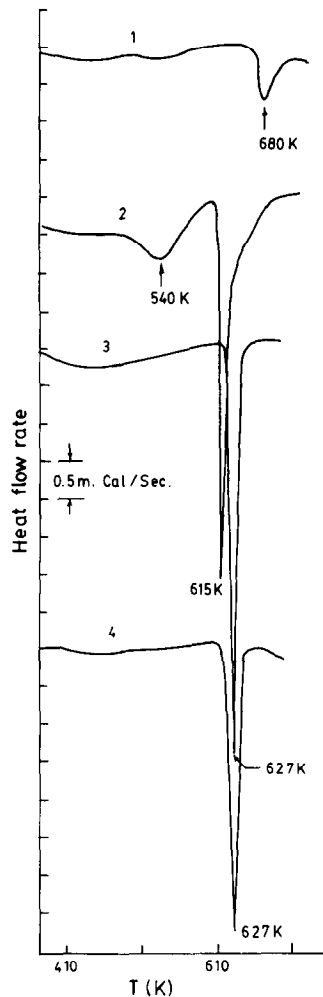


Fig. 3. DSC scans of as-deposited (1) CT-EN (4.3P), scan rate: 20 K min⁻¹; (2) CT-EN (9P), scan rate: 20 K min⁻¹; (3) CT-EN (12.5P), scan rate: 20 K min⁻¹; (4) CT-EN (15.5P), scan rate: 20 K min⁻¹.

with more than 12.5% P. The values of the peak temperature (T_{HP}) and heat evolved (ΔH) derived from thermograms recorded at 10 K min⁻¹ are given in Table 4.

Thermograms of GE-EN deposits (recorded at a scan rate of 20 K min⁻¹) (Fig. 4, curves 5, 6 and 7) are characterized by two irreversible peaks, one at low temperature and one at high temperature. The low-temperature peaks of all three deposits were found to be double peaks. The higher-temperature peak of GD-EN (6.4P) alone was found to be a double peak (Fig. 4, curve 6). Calorimetric data pertaining to these deposits derived from thermograms recorded at 10 K min⁻¹ are also presented in Table 4.

A stress-relief treatment of 350 K for 2 h in vacuum did not eliminate the low-temperature peaks in deposits that showed them. Hence the

TABLE 4. Calorimetric data and peak temperatures for EN (scan rate 10 K min⁻¹)

Deposit	T_{LP1} (K)	T_{LP2} (K)	T_{HP1} (K)	T_{HP2} (K)	ΔH (cal g ⁻¹)
1. CT-EN (4.3P)	-	-	680	-	3.16
2. CT-EN (9P)	540 (a)	-	615 (b)	-	$a - 5.94$ $b - 6.21$
3. CT-EN (12.5P)	-	-	627	-	17.32
4. CT-EN (15.5P)	-	-	627	-	17.49
5. GM-EN (6.4P)	400	525 (a)	645 (b)	-	$a - 9.53$ $b - 9.75$
6. GD-EN (6.4P)	455 (a ₁)	540 (a ₂)	635 (b)	655 (c)	$a_1 + a_2 = 13.65$ $b - 2.52$ $c - 7.22$
7. GT-EN (4.8P)	455 (a)	546 (a)	660 (b)	-	$a - 11.6$ $b - 9.72$

Note: T_{LP1} = temp. of low-temp. peak 1; T_{LP2} = temp. of low-temp. peak 2; T_{HP1} = temp. of high-temp. peak 1; T_{HP2} = temp. of high-temp. peak 2.

low-temperature exotherm is not due to stress relief.

Taking an overall view, one could generalize that DSC of hypoeutectic Ni-P alloy is characterized by two peaks (i.e., a low-temperature peak and a high-temperature peak), while EN with a composition around that of the eutectic exhibits only the high-temperature peak. These peaks may show splitting.

The low-temperature peak

Single or multiple low-temperature peaks have been reported for Ni-P alloy prepared by different methods. Only some of the authors have attempted to identify the process responsible for the low-temperature peak. The following explanations have been suggested:

- (i) The low-temperature peak process is separation of f.c.c. Ni in an amorphous matrix [20-22].
- (ii) The low-temperature peak is due to transformation of amorphous material into a single f.c.c. metastable solid solution of P in Ni [23].
- (iii) The low-temperature peak is due to development of Ni-rich but still amorphous regions [24].

With a view to examining which of these explanations is valid for our results, XRD of the samples was performed after heating the sample at T_{LP} for 15 min (T_{LP} = temperature of low-temperature peak). In the case of samples exhibiting a double peak, the samples were heated at both peak temperatures (T_{LP1} and T_{LP2} ; T_{LP1} = temperature of low-temperature peak 1 and T_{LP2} = temperature of low-temperature peak 2). All of the samples gave diffractograms similar to

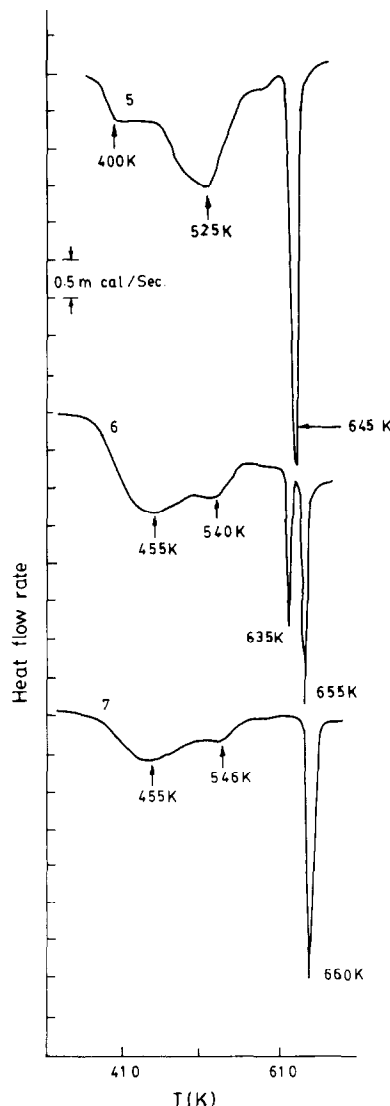


Fig. 4. DSC scans of as-deposited (5) GM-EN (6.4P), scan rate: 20 K min⁻¹; (6) GD-EN (6.4P), scan rate: 20 K min⁻¹; (7) GT-EN (6.4P), scan rate: 20 K min⁻¹.

that shown in Fig. 1(d), i.e., one very broad peak near the Ni(111) peak, and were found to be virtually the same as the XRD pattern of the 'as-plated' deposit (Fig. 1(b)). From the XRD results it is not possible to state anything conclusively regarding the process responsible for the low-temperature peak.

If Ni were to separate out, the magnetic moment of the sample should increase, since nickel phosphides and eutectic Ni-P alloy are non-magnetic. To test this hypothesis, magnetization measurements were carried out on the binary alloys in the as-plated condition as well as after heating at T_{LP} for 15 min.

The variation of magnetization with field of samples in the as-plated condition indicated rel-

atively strong ferromagnetic behaviour in the case of CT-EN (4.3P) (Fig. 5, curve 1) and very weak ferromagnetism for other deposits (Fig. 5, curves 2, 3 and 4; Fig. 6). The saturation magnetic moments (σ_∞) obtained from the above plots are given in Table 5. It is seen that, except for CT-EN (4.3P), all deposits have a very low σ_∞ value. It is surprising that GT-EN (4.8P) shows a saturation magnetic moment of only 0.83 e.m.u. g^{-1} , whereas CT-EN (4.3P), which has a similar P

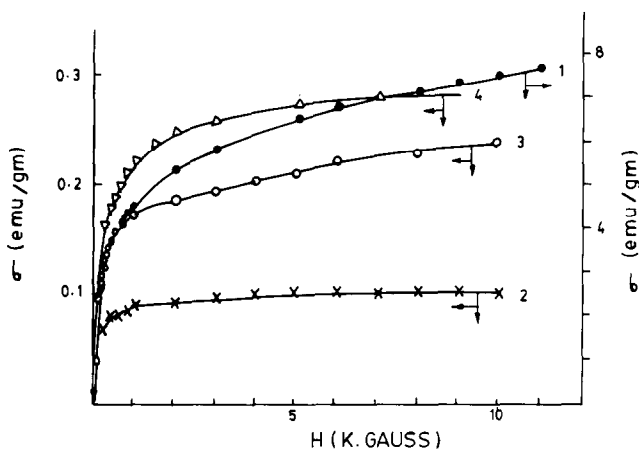


Fig. 5. Variation of magnetic moment with field for as-deposited (1) CT-EN (4.3P); (2) CT-EN (9P); (3) CT-EN (12.5P); (4) CT-EN (15.5P).

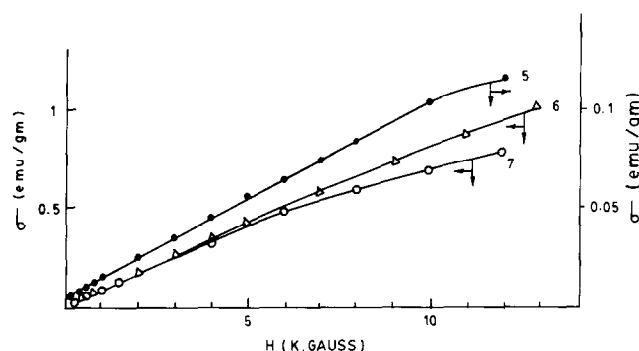


Fig. 6. Variation of magnetic moment with field for as-deposited (5) GM-EN (6.4P); (6) GD-EN (6.4P); (7) GT-EN (4.8P).

TABLE 5. Saturation magnetic moments (σ_∞) of binary EN alloys

Deposit	σ_∞ of as-plated EN (e.m.u. g^{-1})	σ_∞ of EN (e.m.u. g^{-1}) heated for 30 min at:	
		T_{LP1}	T_{LP2}
CT-EN (4.3P)	7.80	—	—
CT-EN (9.0P)	0.11	—	0.68
GM-EN (6.4P)	0.12	—	8.50
GD-EN (6.4P)	0.25	8	13.80
GT-EN (4.8P)	0.83	10	11.20

content, gives a σ_∞ value of 7.8 e.m.u. g^{-1} , i.e., an order of magnitude larger. This observation further strengthens our inference, drawn from XRD patterns of deposits, that GT-EN (4.8P) is perhaps amorphous even though its phosphorus content is small.

Heat treating the deposit at the peak temperature of the low-temperature peak makes its ferromagnetic behaviour stronger (Table 5). Whenever the sample exhibits a double peak it is seen that heat treatment at the second peak temperature (T_{LP2}) increases the value of σ_∞ further, i.e., σ_∞ after heating at T_{LP2} is greater than σ_∞ obtained after heating at T_{LP1} .

In the Ni-P system only Ni is a ferromagnetic phase. Since the deposit becomes distinctly ferromagnetic after heating at the low-temperature peak temperature, we may conclude that heating results in the separation of crystalline Ni. Such precipitated Ni is likely to be saturated with phosphorus.

Randin *et al.* [25] found that Ni precipitated from EN heated at 800 °C showed a lattice constant of $3.5237 \pm 0.0003 \text{ \AA}$, which compared well with the ASTM value of 3.5238 \AA for pure Ni. They argued in the following manner to assess the solubility of P in Ni. Introduction of 0.58 wt.% P (which has the same atomic radius as Cu) into Cu changed its lattice constant from 3.6078 to 3.6092 Å. A much larger change in lattice constant was to be expected for Ni containing a similar percentage of P, because the atomic radius of P is 3% smaller than that of Ni. Since the lattice constant of Ni precipitated from EN exhibited a smaller change than that of the Cu-P system, they concluded that the P content of Ni precipitating out of EN was very low (less than 1 at.%). A similar conclusion was also reached by Vafaei-Makhsos *et al.* [26] from estimation of the amount of P in the separated Ni crystallites by X-ray fluorescence.

From measurements of the Curie temperature (T_c) of the ferromagnetic phase separating out upon heat treatment at low temperature of electrodeposited $Ni_{78}P_{22}$ alloy and the data of Albert *et al.* on the concentration dependence of the Curie temperature in crystalline Ni (P) solid solution [27], Bakonyi *et al.* [19] concluded that the magnetic phase separating out upon low-temperature heat treatment was Ni containing at most 1 at.% P.

In the light of the above literature information, we conclude that the low-temperature peak arises owing to crystallization of Ni saturated with P. The saturation magnetic moment of such a Ni (P)

system will be practically the same as that of pure Ni, as seen from the data of Albert *et al.* [27]. Therefore, an estimate of the amount of Ni separating out as a result of the low-temperature heat treatment can be made by dividing the experimentally observed σ_∞ value by 55. The percentages of Ni calculated by this method are shown in Table 6. It is seen that more Ni separates out at T_{LP2} . This result is similar to the observation made by Bakonyi *et al.* [19]. However, the ΔH values do not appear to show any correlation with the amount of Ni precipitating out. This may perhaps be due to two processes occurring at the low temperature, i.e., crystallization of Ni and reorganization of amorphous matrix. The heat evolved may be due to both of them.

At this stage an interesting question may be raised. How is it that the presence of a significant amount of Ni is not revealed by XRD? A plausible answer to this question is as follows: the peak due to the amorphous material at the position of Ni(111) reflection is so broad that it covers all the strong reflections of Ni. The diffraction pattern due to Ni precipitating at T_{LP} is likely to be broad, owing to the small particle size, and hence might be obscured by the peak due to the amorphous matrix.

Multiple peaks (2 or 3 peaks) in the low-temperature transformation of EN have been reported by others [19, 24]. They were interpreted as indicative of a multi-stage process [24]. Bakonyi *et al.* [19] showed that in each of these multiple peaks crystallization of Ni proceeds. Our work also points out the same. Lanzoni *et al.* [22] felt that heterogeneities contribute to splitting of the low-temperature peak.

The fact that peaks occur at similar temperatures for the same process of crystallization of Ni indicates that the crystallization proceeds with more than one activation energy, which is perhaps a

consequence of the presence of more than one local order. It is difficult to state whether different local arrangements exist in the as-plated condition, i.e., heterogeneities or the amorphous matrix rearranges to a different local order with a slightly higher stability, during crystallization of Ni. The work of Bennett and co-workers [28, 29] indicates the existence of at least two (amorphous) local structures.

In the light of the above discussion, it may be concluded that the low-temperature peak(s) seen in the thermograms arise from crystallization of Ni and probably reorganization of the amorphous matrix.

The high-temperature peak

The thermograms of the deposits studied here show only a single peak in the high-temperature region. Thermal data pertaining to this peak are given in Table 4.

The XRD pattern of the deposit after heating for 60 min at T_{HP} (T_{HP} =temperature of high-temperature peak) shows the presence of two crystalline phases, f.c.c. Ni and b.c.t. Ni_3P . This feature is common to all the deposits studied here. The higher-temperature peak may therefore be ascribed to the formation of Ni and Ni_3P . This is in agreement with the results published by several authors [8, 12, 17–25]. Some authors [20, 22, 23] have reported an additional high-temperature peak at about 675 K and ascribed it to the growth of Ni_3P . In the present study this peak was not seen. The crystallization and growth peaks probably coincided.

The high-temperature peak of the hypoeutectic alloy GD-EN (6.4P) tends to split into two. This may be due to differences in the activation energy for crystallization from partially crystallized matrix and amorphous matrix.

It is seen that the saturation magnetic moment of deposits heated for 30 min at T_{HP} (Table 7) are smaller than what might be expected if one regarded the deposit as a mixture of Ni and Ni_3P . For calculating σ_∞ , the solubility of P in Ni was assumed to be zero, since literature reports indicate that it is much smaller than 0.5 wt.% [15, 19, 25]. If the solubility of P is larger it will only increase the calculated value of σ_∞ , since Ni bound as Ni_3P will decrease. From the above discussion it may be inferred that the crystallization process is not completed in 30 min by holding the temperature at T_{HP} . Bakonyi *et al.* [19] have made a similar observation. Mahoney and Dynes [30] also point out that a very long time is needed to complete crystallization. A further interesting observation

TABLE 6. Amount of crystalline nickel separating out as a result of heat treatment for 30 min at T_{LP} (calculated from σ_∞)

Deposit	Temp. ^a (K)	% Ni in EN after heat treatment ^b	ΔH (cal g ⁻¹)
CT-EN (9P)	540.0	16.4	5.94
GM-EN (6.4P)	525.0	15.5	9.53
GD-EN (6.4P)	455.0	14.5	10.95
GD-EN (6.4P)	540.0	25.1	2.70
GT-EN (4.8P)	455.0	18.2	9.18
GT-EN (4.8P)	546.0	20.4	2.42

^aSamples were heated at this temp. for 30 min.

^bCalculated from σ_∞ using a value of 55 e.m.u. g⁻¹ for pure Ni.

TABLE 7. Comparison of saturation magnetic moment of EN heated for 30 min at T_{HP} and saturation magnetic moment expected on the basis of a Ni + Ni₃P mixture

Deposit	σ_{∞} of deposit heated at T_{HP} for 30 min (e.m.u. g ⁻¹)	σ_{∞} calculated ^a (e.m.u. g ⁻¹)
CT-EN (4.3P)	31.40	39.19
CT-EN (9P)	11.50	21.95
CT-EN (12.5P)	6.50	9.05
CT-EN (15.5P)	5.10	10.00
GM-EN (6.4P)	19.00	31.56
GD-EN (6.4P)	18.60	31.56
GE-EN (4.8P)	26.00	37.34

^aAll the P is assumed to be Ni₃P. σ_{∞} of Ni is taken as 55 e.m.u. g⁻¹. It is assumed that only Ni contributes to the σ_{∞} of the mixture.

TABLE 8

Crystallization temperatures T_{HP} and total ΔH (ΔH_T) of EN deposited from ethanolamine baths

Deposit	T_{HP} ^{a, b} (K)	ΔH_T ^a (cal g ⁻¹)
CT-EN (4.3P)	680	3.16
CT-EN (9P)	615	12.15
CT-EN (12.5P)	627	17.32
CT-EN (15.5P)	627	17.49
GM-EN (6.4P)	645	19.28
GD-EN (6.4P)	655	23.30
GT-EN (4.8P)	660	21.32

^aObtained from thermograms recorded at a scan rate of 10 K min⁻¹.

^bThe temperatures correspond to the second peak whenever the peak is a double peak.

by these authors is that DSC peaks are obtained at progressively lower temperatures on samples thermally aged for increasing times. This probably shows that the crystallization is not complete at the temperature corresponding to the termination of the DSC peak.

It is generally expected that the total ΔH (i.e., the sum of the ΔH values of all the peaks) should increase with increasing phosphorus content of the deposit [19]. The total ΔH of the thermograms of CT-EN deposits is seen to follow this trend (Fig. 7), whereas the values for deposits from GE baths do not fall on the curve. Deposits from GE baths exhibit amorphous structure even at lower phosphorus contents and therefore the ΔH values are also larger.

Another trend reported in the literature is that the peak temperature of the high-temperature peak (often called the crystallization temperature) decreases with increasing phosphorus content, except

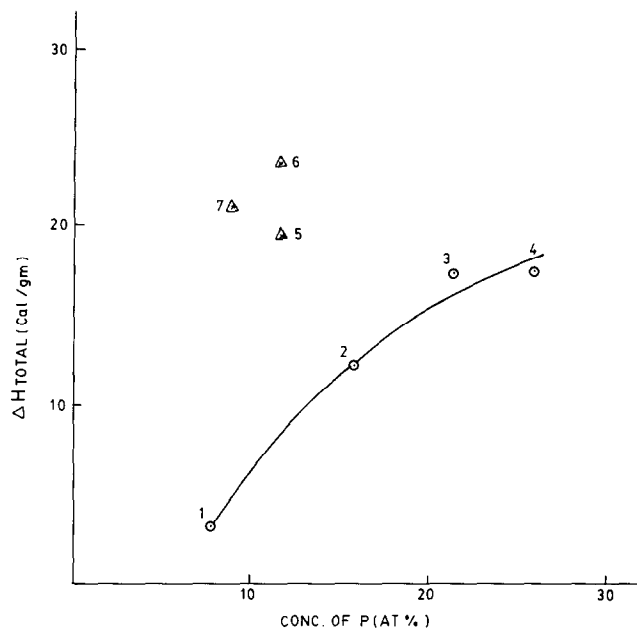


Fig. 7. ΔH_{total} vs. P content of EN deposited from ethanolamine baths. The numbers 1-7 refer to the deposit numbers (Table 3).

for the slight increase around the eutectic concentration of about 19 at.% [18, 19]. From the data in Table 8 it is seen that this trend is followed by CT-EN deposits. However, GE-EN deposits behave as exceptions. This again shows that these deposits are very different structurally. They are probably more loosely packed, with a large number of voids.

Conclusions

Except for the 4.3% P deposit, all the EN deposits studied here gave an XRD pattern characterized by a broad peak centred around the Ni(111) peak and a very weak secondary peak (also broad) at higher 2θ . The peak position varied with the composition of the deposit. These observations were consistent with the interpretation that the deposits were amorphous at P contents greater than 9% in the case of CT-EN. Deposits of GT-EN, on the other hand, exhibited an amorphous character even at 4.8% P. The lower density of EN deposits from the glycine bath as compared with CT-EN of the same P content is consistent with the above XRD result. This shows that the P concentration needed to amorphize the deposit depends on the bath chemistry.

All the deposits, upon heat treatment at 400 °C (673 K), transformed into a mixture of crystalline Ni and Ni₃P. This result supports the conclusion that all these EN deposits exhibit higher hardness

upon heat treatment owing to a precipitation hardening mechanism.

All the deposits gave only exothermic peaks in the DSC study. Hypoeutectic deposits (i.e., those with a phosphorus content of less than 20 at.%) showed two exothermic transformations. The low-temperature transformation was shown here by magnetic measurements to be due to separation of nickel or a nickel-rich phase in an amorphous matrix. The higher-temperature transformation was found to be due to crystallization of the amorphous matrix into Ni + Ni₃P. The deposit with 25 at.% P also transformed in a single step, but yielded a small amount of Ni besides Ni₃P, which may be interpreted as due to non-stoichiometry of Ni₃P.

Acknowledgements

The authors thank Dr C. Balasingh for his help in recording XRD patterns of samples, Dr Sudha Mahadevan and Mr A. Giridhar for recording DSC patterns, and RSIC, Indian Institute of Technology, Madras, for magnetic measurements.

References

- 1 K. S. Rajam and S. R. Rajagopalan, *Tech. Mem. MT-TM-8601*, 1986.
- 2 K. S. Rajam and S. R. Rajagopalan, *Tech. Mem. MT-TM-8801*, 1988.
- 3 K. S. Rajam, I. Rajagopal and S. R. Rajagopalan, *Met. Finish.*, 88 (1990) 41; 88 (1990) 77.
- 4 W. H. Safranek, *The Properties of Electrodeposited Metals and Alloys*, Elsevier, Amsterdam, 1974, p. 479.
- 5 *ASTM Powder Diffraction File Inorganic (Set 1-5)*, Joint Committee on Powder Diffraction Standards, Philadelphia, PA, 1967, p. 587.
- 6 A. H. Graham, R. W. Lindsay and H. J. Read, *J. Electrochem. Soc.*, 112 (1965) 401.
- 7 S. L. Chow, N. E. Hedgecock and M. Schlesinger, *J. Electrochem. Soc.*, 119 (1972) 1614.
- 8 U. Pittermann and S. Ripper, in S. Steeb and H. Warlimont (eds.), *Rapidly Quenched Metals*, Elsevier, Amsterdam, 1985, pp. 385-388.
- 9 A. W. Goldenstein, W. Rostoker and F. Schossberger, *J. Electrochem. Soc.*, 104 (1957) 104.
- 10 G. S. Cargill III, *J. Electrochem. Soc.*, 41 (1970) 12.
- 11 G. S. Cargill III, in I. Hargittai and W. J. Orville-Thomas (eds.), *Diffraction Studies on Non-crystalline Substances*, Elsevier, New York, 1981, pp. 733-780.
- 12 B. G. Bagley and D. Turnbull, *J. Appl. Phys.*, 39 (1968) 5681.
- 13 B. D. Cullity, *Elements of X-ray Diffraction*, Addison-Wesley, Reading, MA, 1959, pp. 388-390.
- 14 C. E. Higgs, *Electrodeposition Surf. Treat.*, 2 (1973/74) 315.
- 15 E. Vafaei-Makhsos, *J. Appl. Phys.*, 51 (1980) 6366.
- 16 K. H. Kuo, Y. K. Wu, J. Z. Liang and Z. H. Lai, *Philos. Mag. A*, 51 (1985) 205.
- 17 U. Pittermann and S. Ripper, *Z. Metallkd.*, 74 (1983) 783.
- 18 U. Pittermann and S. Ripper, *Phys. Status Solidi*, 93 (1986) 131.
- 19 I. Bakonyi, A. Cziraki, T. Nagi and M. Hosso, *Z. Metallkd.*, 77 (1986) 425.
- 20 M. Allen and B. Vander Sande, *Scr. Metall.*, 16 (1982) 1161.
- 21 M. S. Grewal, S. A. Sastri and B. H. Alexander, *Thermochim. Acta*, 14 (1976) 25.
- 22 E. Lanzoni, G. Poli and G. Centi, *J. Therm. Anal.*, 29 (1984) 701.
- 23 W. G. Clements and B. Canotot, in N. J. Grant and B. G. Giessen (eds.), *Rapidly Quenched Metals*, MIT Press, Cambridge, MA, 1976, p. 267.
- 24 A. Cziraki, B. Fogarassy, I. Bakonyi, K. Tompa, T. Bagi and Z. Hegedus, *J. Phys. (Paris)*, C8-141 (1980) 41.
- 25 J. P. Randin, P. A. Maire, E. Saurer and H. E. Hintermann, *J. Electrochem. Soc.*, 114 (1967) 442.
- 26 E. Vafaei-Makhsos, Edwin L. Thomas and Louis E. Toth, *Metall. Trans. A*, 9 (1978) 1449.
- 27 P. A. Albert, Z. Kovac, H. R. Lilienthal, T. R. McGurie and V. Nakamura, *J. Appl. Phys.*, 38 (1967) 1258.
- 28 D. S. Lashmore, L. H. Bennett, H. E. Schone, P. Gustafson and R. E. Watson, *Phys. Rev. Lett.*, 48 (1982) 1760.
- 29 L. H. Bennett, H. E. Schone and P. Gustafson, *Phys. Rev. B*, 18 (1978) 2027.
- 30 M. W. Mahoney and P. J. Dynes, *Scr. Metall.*, 19 (1985) 539.